VOLUME 121, NUMBER 11
MARCH 24, 1999

JOURNAL OF THE AMERICAN CHEMICAL SOCIETY

Rubredoxin Variant Folds without Iron

Pavel Strop[†] and Stephen L. Mayo*[,‡]

Contribution from Biochemistry Option and Howard Hughes Medical Institute and Division of Biology, California Institute of Technology, Mail Code 147-75, Pasadena, California 91125

Received October 1, 1998

Abstract: *Pyroccocus furiosus* rubredoxin (PFRD), like most studied hyperthermophilic proteins, does not undergo reversible folding. The irreversibility of folding is thought to involve PFRD's iron-binding site. Here we report a PFRD variant (PFRD-XC4) whose iron binding site was redesigned to eliminate iron binding using a computational design algorithm. PFRD-XC4 folds without iron and exhibits reversible folding with a melting temperature of 82 °C, a thermodynamic stability of 3.2 kcal mol^{-1} at 1 °C, and NMR chemical shifts similar to that of the wild-type protein. This variant should provide a tractable model system for studying the thermodynamic origins of protein hyperthermostability.

Introduction

Hyperthermophilic proteins have attracted considerable attention because they can serve as model systems for the determination of factors responsible for protein stability. These include an optimized use of structure elements such as hydrophobic interactions, packing forces, hydrogen bonds, and salt bridges.[1−5] In most cases, however, the usual methods for determining thermodynamic stability cannot be used for hyperthermophilic proteins. The measurement of protein stability requires reversible folding, but in almost all studied hyperthermophilic proteins, the denaturation is not reversible.[6−8] In the few hyperthermophilic proteins that exhibit reversible folding, there are other elements that complicate the determination of the free energy of folding. These proteins either are dimeric[9,10] or do not fit a two-state denaturation model.[10] Irreversible denaturation has been addressed by hydrogen exchange studies[11] and by molecular dynamics simulations,[12] but neither of these methods provides an accurate measure of free energy.

Rubredoxins are small (∼6 kDa) iron−sulfur proteins with the active site arranged around an iron tetrahedrally coordinated to four cysteinate sulfurs (Figure 1a). Thirteen rubredoxins have

[†] Biochemistry Option.
[‡] Howard Hughes Medical Institute and Division of Biology. E-mail: steve@mayo.caltech.edu.

(1) Lee, B.; Vasmatzis, G. *Curr. Opin. Biotechnol.* **1997**, *8*, 423−428.
(2) Straume, M., Murphy, K. P., Freire, E., Adams, M. W. W., Kelly, R. M., Eds. *Thermodynamic Strategies for Protein Design—Increased Temperature Stability*; American Chemical Society: Washington, DC, 1992; Vol. 498, pp 122−135.
(3) Rees, D. C.; Adams, M. W. W. *Structure* **1995**, *3*, 251−254.
(4) Eidsness, M. K.; Richie, K. A.; Burden, A. E.; Kurtz, J., D. M.; Scott, R. A. *Biochemistry* **1997**, *36*, 10406−10413.
(5) Jiang, X.; Bishop, E. J.; Farid, R. S. *J. Am. Chem. Soc.* **1997**, *119*, 838−839.
(6) Cavagnero, S.; Zhou, Z.; Adams, M.; Chan, S. *Biochemistry* **1998**, *37*, 3377−3385.
(7) Klump, H. H.; W, A. M. W.; Robb, F. T. *Pure Appl. Chem.* **1994**, *66*, 485−489.
(8) Wampler, E. J.; Neuhaus, B. E. *J. Protein Chem.* **1997**, *16*, 721−732.
(9) Li, W.; Grayling, R. A.; Sandman, K.; Edmonson, S.; Shriver, J. W.; Reeve, J. N. *Biochemistry* **1998**, *37*, 10563−10572.
(10) MacBeath, G.; Kast, P.; Hilvert, D. *Biochemistry* **1998**, *37*, 10062−10073.
(11) Hiller, R.; Zhou, Z.; Adams, M.; Englander, W. *Proc. Natl. Acad. Sci.* **1997**, 11329−11332.
(12) Bradley, A. E.; Stewart, E. D.; Adams, W. M.; Wampler, J. E. *Protein Sci.* **1993**, 650−665.

10.1021/ja9834780 CCC: $18.00
Published on Web 03/05/1999

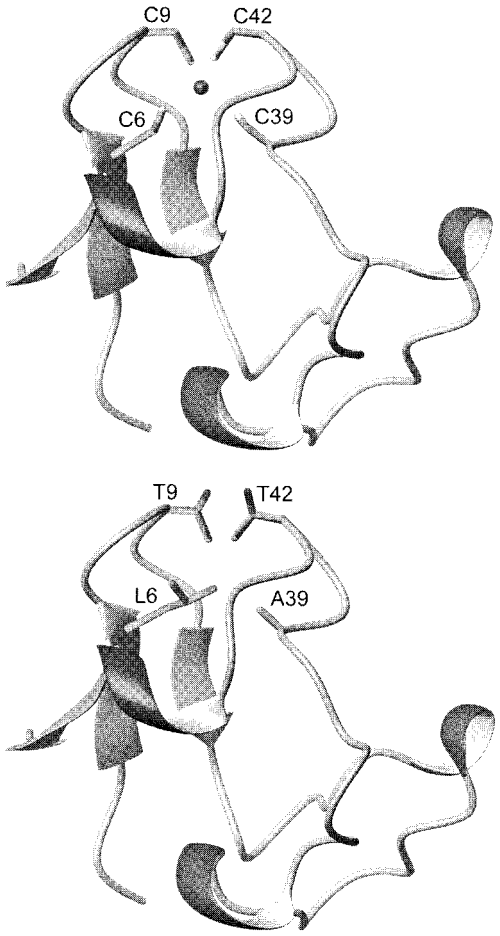

Figure 1. (a) Ribbon diagram of wild-type mesophilic *Desulfovibrio vulgaris* rubredoxin showing the four cysteine residues that coordinate the iron. (b) Ribbon diagram showing the computed side chain orientations of the four mutations. Structure figures were generated using MOLMOL.[41]

been sequenced, and all conserve the four cysteine ligands (residues 5, 8, 38, and 41 in the hyperthermophilic *Pyroccocus furiosus* rubredoxin (PFRD) and residues 6, 9, 39, and 42 in the mesophilic *Desulfovibrio vulgaris* rubredoxin (DVRD)). Since several rubredoxin structures are available from the Brookhaven Protein Data Bank at resolutions of 0.95−1.8 Å,[13−19] these proteins are valuable models for the investigation of the origins of thermostability.

It is believed that the iron binding site in rubredoxin is the cause of irreversible unfolding.[20] Here we report a *Pyroccocus furiosus* rubredoxin variant (PFRD-XC4) which was designed to eliminate the iron-binding site using a computational design algorithm. PFRD-XC4 is able to fold in the absence of iron and undergoes reversible denaturation. The variant provides an excellent opportunity for systematic exploration of the factors determining protein thermostability.

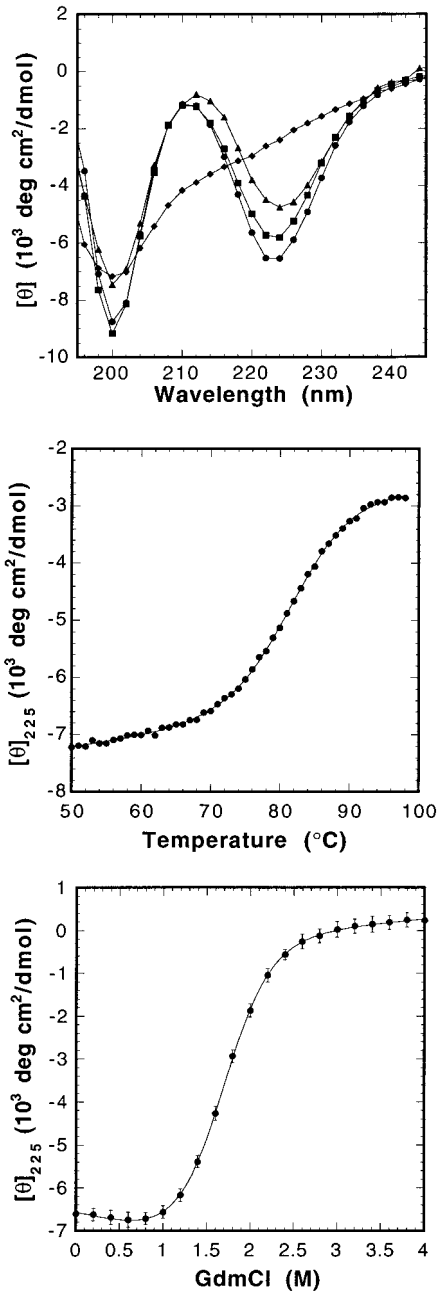

Figure 2. Circular dichroism measurements of wild-type *Pyroccocus furiosus* rubredoxin (PFRD) and the PFRD-XC4 variant. (a) Wavelength scans of PFRD-XC4 at 1 °C (circles), 99 °C (diamonds), and refolded at 1 °C (squares). PFRD is also shown at 1 °C for comparison (triangles). (b) Thermal unfolding curve for PFRD-XC4 monitored by CD at 225 nm. (c) Guanidinium chloride denaturation curve for PFRD-XC4 at 1 °C.

Experimental Section

Computational Modeling. In the calculation using a mesophilic structure, the four cysteine residues that form rubredoxin's iron binding site were optimized in the absence of iron coordination. Two of the cysteines were classified as core residues (Cys^6 and Cys^{39}) and two as boundary residues (Cys^9 and Cys^{42}). Residues were classified into core, surface, and boundary groups as previously described.[21] Seven amino acid types (Ala, Val, Leu, Ile, Phe, Tyr, and Trp) were considered at the two core positions, and 16 amino acid types (Ala, Val, Leu, Ile,

(13) Bernstein, F. C.; Koetzle, T. F.; Williams, G. J. B.; Meyer Jr, E. F.; Brice, M. D.; Rodgers, J. R.; Kennard, O.; Shimanouchi, T.; Tasumi, M. *J. Mol. Biol.* **1977**, *112*, 535−542.
(14) Adman, E. T.; Sieker, L. C.; H, J. L. *J. Mol. Biol*. **1991**, 337−352.
(15) Dauter, Z.; Sieker, L.; Wilson, K. *Acta Crystallogr*. **1992**, 42−59.
(16) Day, M.; Hsu, B.; Joshua-tor, L.; Park, J.; Zhou, Z.; Adams, M.; Rees, D. *Protein Sci.* **1992**, 1494−1507.
(17) Frey, M.; Sieker, L. C.; Payan, F.; Haser, R.; Bruschi, M.; Pepe, G.; LeGall, J. *J. Mol. Biol*. **1987**, 525−541.
(18) Sieker, L. C.; Stenkamp, R. E.; Jensen, L. H.; Prickril, B.; LeGall, J. *FEBS* **1986**, 73−76.
(19) Watenpaugh, K. D.; Sieker, L. C.; Jensen, L. H. *J. Mol. Biol.* **1979**, 509−522.
(20) Cavagnero, S.; Debe, D.; Zhou, Z.; Adams, M.; Chan, S. *Biochemistry* **1998**, 3369−3376.
(21) Dahiyat, B. I.; Mayo, S. L. *Science* **1997**, *278*, 82−87.

Table 1. ^{1}H NMR Chemical Shifts for PFRD-XC4, pH 6.3, 25 °C[a]

residue		HN	H_α	H_β	others
1	Ala				
2	Lys	8.68	5.45	1.62	HE, 2.92
3	Trp	9.39	4.95	2.74	HD1, 6.87; HE1, 9.73; HE3, 6.61; HZ2, 7.58; HZ3, 6.94; HH2, 7.21
4	Val	9.97	5.57		HG1, 0.78; HG2, 0.93
5	Leu	8.85	4.35	0.16, 1.91	HG, 1.21; HD1, 0.53; HD2, 0.70
6	Lys	9.09	3.79		HG1, 1.41; HG2, 1.57; HE1, 2.86; HE2, 2.95; HD, 1.71
7	Ile	8.25	4.09	1.88	
8	Thr	6.92	4.73	4.47	HG2, 1.19
9	Gly	8.72	3.47, 4.24		
10	Tyr	7.59	4.27	2.70, 3.30	HD, 7.33; HE, 7.20
11	Ile	7.34	4.97	1.49	HG2, 0.71; HD1, 0.80; HG1, 1.79
12	Tyr	9.53	4.64	2.92, 3.17	HD, 7.10; HE, 6.43
13	Asp	8.78	4.92	2.26, 2.86	
14	Glu	8.26	3.86	1.94, 2.11	HG, 3.03
15	Asp	8.03	4.27		
16	Ala	7.2	4.35	1.49	
17	Gly	8.12	3.59, 3.98		
18	Asp	8.32	5.17	3.01	
19	Pro				
20	Asp	9.09	4.5	2.75	
21	Asn	7.73	5.19	2.69, 3.16	
22	Gly	7.83	3.86, 4.15		
23	Ile	7.67	4.38	1.94	HG2, 0.91; HD1, 0.82; HG1, 1.34
24	Ser	8.72	4.61	3.74, 3.90	
25	Pro				
26	Gly	8.22	3.74, 4.25		
27	Thr	7.3	4.01	3.94	HG1, 6.35; HG2, 1.04
28	Lys	8.92	4.01	1.50, 2.12	HD, 1.69; HE, 3.09
29	Phe	10.06	3.29		HZ, 6.52; HD, 5.70; HE, 6.12
30	Glu	9.34	3.72	1.92, 2.08	HG1, 2.21; HG2, 2.32
31	Glu	7.41	4.09	2.06, 2.20	
32	Leu	6.86	3.88	0.34, 0.88	HG, 0.70; HD2, −0.14
33	Pro				
34	Asp	8.76	4.25	2.59, 2.69	
35	Asp	8.23	4.53	2.58, 2.87	
36	Trp	7.7	4.15	2.97	HD1, 7.19; HE1, 10.41; HE3, 6.84; HZ2, 7.49; HZ3, 6.25; HH2, 7.00
37	Val	6.72	4.32		HG1, 1.33
38	Ala	8.49		1.28	
39	Pro		4.13	1.70, 2.27	HD1, 2.76; HD2, 3.48; HG, 1.90
40	Ile				
41	Thr				
42	Gly	7.62	3.64, 3.86		
43	Ala	8.88	4.19		
44	Pro				
45	Lys	6.92		2.19, 2.39	HG1, 1.00; HG2, 1.18; HD, 1.70
46	Ser	8.12	4.38	4.03, 4.19	
47	Glu	8.04	4.48	1.98, 2.32	
48	Phe	8.16		4.94, 3.76	
49	Glu	9.34	4.93		
50	Lys	8.55	3.2	1.12, 1.28	HG1, 0.07; HG2, 0.22; HD, 0.65; HE, 2.68
51	Leu	8.68	4.3	1.29, 1.48	HD, 0.83
52	Glu	8.1	4.35	1.84	HG1, 2.07; HG2, 2.19
53	Asp	8.03	4.34	2.49, 2.65	

[a] Chemical shifts were referenced to H_2O (4.77 ppm at 25 °C).

Phe, Tyr, Trp, Ser, Thr, Asp, Asn, Glu, Gln, His, Lys, and Arg) were considered at the two boundary positions. Both amino acid identities and side chain conformations were determined by the algorithm for the four optimized residues. Neighboring residues 7, 10, 40, and 43 were fixed in identity, but their conformations were allowed to change in the calculation. All other residues as well as the backbone were held fixed. Computational details, potential functions, and parameters for van der Waals, solvation, and hydrogen bonding are described in our previous work.[21−26]

Mutagenesis and Protein Purification. The hyperthermophilic mutant PFRD-XC4 was constructed by inverse PCR[27] using a synthetic *Pyroccocus furiosus* rubredoxin gene in plasmid pt7-7.[4] The mutations for PFRD-XC4 are C5L, C8T, C38A, and C41T. A synthetic gene based on the sequence of the *Desulfovibrio vulgaris* rubredoxin was constructed for the mesophilic variant (DVRD-XC4) by recursive PCR[28] and cloned into pt7-7. The mutations for DVRD-XC4 are C6L, C9T, C39A, and C42T. Both mutants were verified by sequencing. Recombinant proteins were expressed by IPTG induction in BL21(DE3) hosts (Invitrogen) as described[29] and isolated using a freeze/thaw method.[30] Purification was accomplished by reverse-phase high-performance liquid chromatography using first a linear 1%/min followed by a 0.07%/min acetonitrile/water gradient containing 0.1% TFA. Molecular weights were verified by mass spectrometry.

(22) Dahiyat, B. I.; Mayo, S. L. *Protein Sci.* **1996**, *5*, 895−903.
(23) Dahiyat, B. I.; Sarisky, C. A.; Mayo, S. L. *J. Mol. Biol.* **1997**, *273*, 789−796.
(24) Dahiyat, B. I.; Mayo, S. L. *Proc. Natl. Acad. Sci. U.S.A.* **1997**, *94*, 10172−10177.
(25) Dahiyat, B. I.; Gordon, D. B.; Mayo, S. L. *Protein Sci.* **1997**, *6*, 1333−1337.
(26) Malakauskas, S. M.; Mayo, S. L. *Nat. Struct. Biol.* **1998**, *5*, 470−475.
(27) Hemsley, A.; Arnheim, N.; Toney, M. D.; Cortopassi, G.; Galas, D. J. *Nucleic Acids Res.* **1989**, *17*, 6545−6551.
(28) Prodromou, C.; Pearl, L. H. *Protein Eng.* **1992**, *5*, 827−829.
(29) Alexander, P.; Fahnestock, S.; Lee, T.; Orban, J.; Bryan, P. *Biochemistry* **1992**, *31*, 3597−3603.
(30) Johnson, B. H.; Hecht, M. H. *Bio/Technology* **1994**, *12*, 1357−1360.

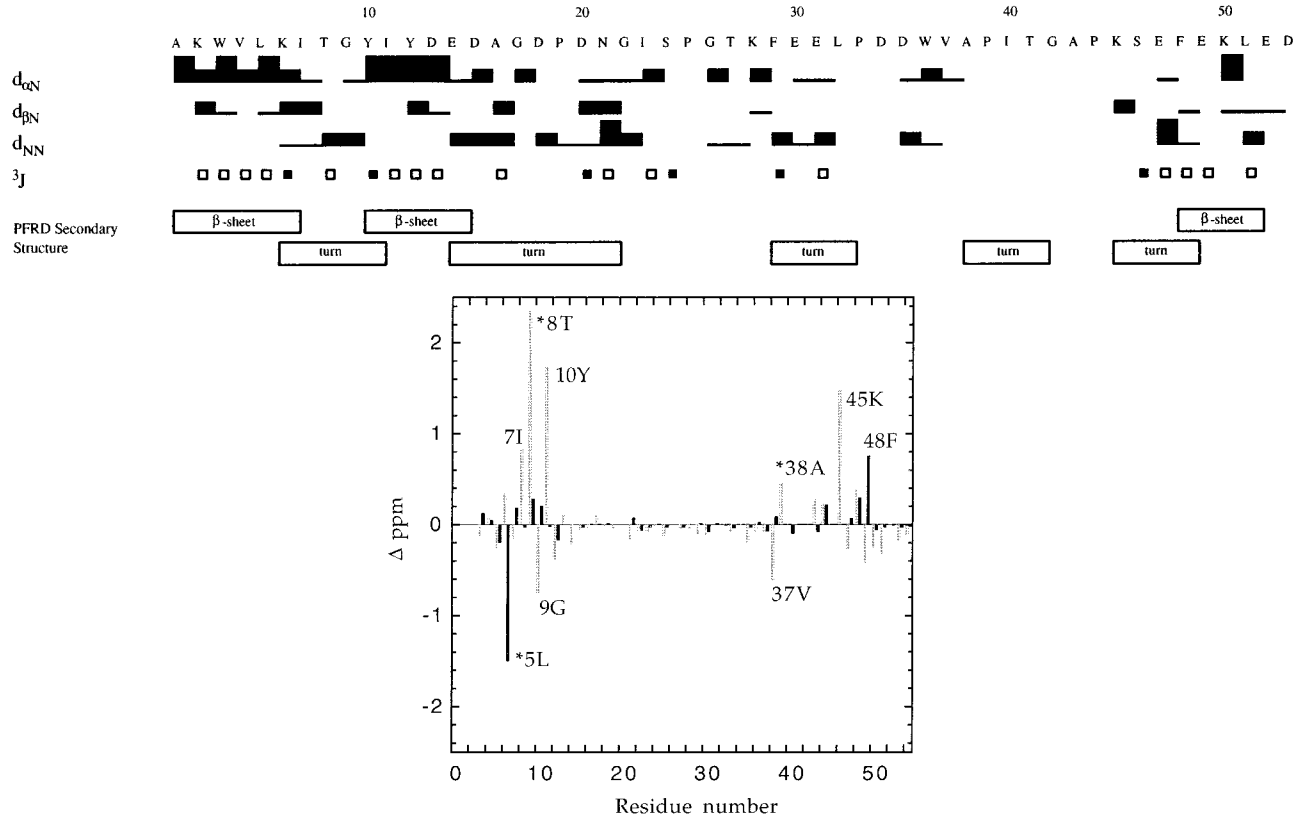

Figure 3. (a) NMR assignments summary and NOE connectivities of PFRD-XC4. Bars represent unambiguous connectivities with bar thickness indexed to the intensity of the resonance. Coupling constants with $^3J_{HNHA} > 8.0$ Hz are shown as open squares, and $^3J_{HNHA} < 4.0$ Hz are shown as black squares. Secondary structural elements of PFRD are given at the bottom of the figure for comparison.[42] (b) Chemical shift difference between PFRD and PFRX-XC4 for amide nitrogen (black lines) and α hydrogens (shaded line). Proline residues 19, 25, 33, 39, and 44 not shown. Residues 40 and 41 also not shown due to a missing sequential assignments. Mutations are at positions 5, 8, 38, and 41. Residues 7, 9, 10, and 48 are in the close proximity of the mutated site.

CD Analysis. CD data were collected on an Aviv 62DS spectrometer equipped with a thermoelectric unit and using a 1 mm path length cell. Protein samples were 40 μM in 50 mM sodium phosphate buffer at pH 6.3. Concentrations were determined by UV spectrophotometry. Thermal melts were monitored at 225 nm. Data were collected every 2 °C with an equilibration time of 2 min and an averaging time of 10 s. T_m was determined by fitting the melting curves to a two-state model as described.[31] Guanidinium chloride denaturations were performed at 1 °C. ΔG's, *m* values, and error estimates were obtained by fitting the denaturation data to a two-state transition as described.[32]

NMR Studies. NMR data were collected on a Varian Unity Plus 600 MHz spectrometer equipped with a Nalorac inverse probe with a self-shielded *z* gradient. NMR samples were prepared in 90/10 H_2O/D_2O or 99.9% D_2O with 200 mM NaCl and 25 mM acetate-d_3, pH 6.3. The sample concentration was approximately 1.5 mM. Sequential assignment of resonances was achieved by the standard homonuclear method.[33] Two-dimensional DQF-COSY,[34] TOCSY,[35] and NOESY[36] spectra were acquired at 25 °C. The TOCSY spectrum was recorded with a 80 ms mixing time using a clean-MLEV17 mixing sequence. The NOESY spectrum was acquired with a 150 ms mixing time. Water suppression was accomplished either with presaturation during the relaxation delay or with pulsed field gradients.[37] Spectra were processed with VNMR (Varian Associates) and were assigned with ANSIG.[38] $^3J_{HNHA}$ values were derived from NOESY cross-peak fine structure using the INFIT module of XEASY.[39]

Results and Discussion

Backbone coordinates for the mesophilic rubredoxin structure used in the calculations were obtained from Brookhaven Protein Data Bank entry 8rxn.[13,15] A radius scale factor of 0.9 for the van der Waals interactions[24] resulted in two threonine residues at the boundary positions and two alanine residues at the core positions. To obtain an alternate sequence that provides greater core volume, selection for the core positions in the calculation was repeated with the radius scale factor decreased to 0.7 and boundary positions 9 and 42 fixed as threonines. The amino acid sequence selected by the algorithm under these conditions contains the following mutations: C6L, C9T, C39A, and C42T (Figure 1b). The equivalent mutations for the hyperthermophilic variant, PFRD-XC4, are C5L, C8T, C38A, and C41T.

The far-ultraviolet circular dichroism (CD) spectrum of PFRD-XC4 is nearly identical to that of the wild-type protein at 1 °C (Figure 2a). Wavelength scans performed at 1 °C, 99 °C, and then again at 1 °C demonstrate reversible folding (Figure 2a). Thermal denaturation of the variant, monitored by CD at 225 nm, shows a cooperative unfolding transition with a melting temperature (T_m) of 82 °C (Figure 2b). Based on the estimated T_m for the wild-type hyperthermophilic rubredoxin,[11] PFRD-XC4 is destabilized by about 80 °C. The mesophilic variant,

(31) Minor, D. L.; Kim, P. S. *Nature* **1994**, *371*, 264−267.
(32) Santoro, M. M.; Bolen, D. W. *Biochemistry* **1988**, *27*, 8063−8068.
(33) Wüthrich, K. *NMR of Proteins and Nucleic Acids*; John Wiley and Sons: New York, 1986.
(34) Piantini, U.; Sorensen, O. W.; Ernst, R. R. *J. Am. Chem. Soc.* **1982**, *104*, 6800−6801.
(35) Bax, A.; Davis, D. G. *J. Magn. Reson.* **1986**, *65*, 355−360.
(36) Jeener, J.; Meier, B. H.; Bachmann, P.; Ernst, R. R. *J. Chem. Phys.* **1979**, *71*, 4546−4553.
(37) Piotto, M.; Saudek, V.; Sklenar, V. *J. Biomol. NMR* **1992**, *2*, 661−665.
(38) Kraulis, P. J. *J. Magn. Reson.* **1989**, *24*, 627−633.
(39) Bartels, C.; Xia, T. H.; Billeter, M.; Guntert, P.; Wuthrich, K. *J. Biol. NMR* **1995**, *5*, 1−10.

DVRD-XC4, was also expressed and found to be unfolded at 1 °C. Chemical denaturation of PFRD-XC4 at 1 °C using guanidinium chloride (GdmCl), monitored by CD at 225 nm, yielded a free energy of unfolding (ΔG_u) of 3.2 ± 0.1 kcal mol^{-1} and a *m* value of 2.0 kcal mol^{-1} M^{-1} (Figure 2c).

Sequential assignments were obtained for 90% of backbone hydrogens (Table 1). On the basis of the chemical shifts for the amide and α hydrogens, the PFRD-XC4 variant adopts a fold similar to that of PFRD.[40] Chemical shift differences between PFRD and PFRD-XC4 are shown in Figure 3b. The chemical shifts of PFRD-XC4 residues that are distal from the site of mutation do not deviate significantly from those of PFRD, suggesting that these residues are in the same chemical environment as in PFRD. The chemical shifts of residues 7, 9, 10, and 48 significantly diverge from the corresponding PFRD chemical shifts. These residues are expected to have different chemical shifts because they are in close proximity to the mutated site. Lysine 45 does not make a direct contact with the mutated site but makes contact with residues 10 and 48. Examination of NOE sequential connections (Figure 3a) reveals strong HN−HA cross-peaks present in the β-sheet regions (residues 1−6, 10−14, and 49) and HN−HN cross-peaks in the turn regions (residues 6−10, 18−22, 29−32, and 46−47). Large coupling constants ($^3J_{HNHA} > 8.0$ Hz) are also observed for most of the β-sheet residues (Figure 3a). These observations provide additional evidence that PFRD-XC4 adopts a fold similar to that of PFRD.

Given that PFRD-XC4 adopts a fold similar to that of PFRD and undergoes reversible unfolding, it should provide a tractable model system for determination of protein hyperthermostability. PFRD-XC4 should be amenable to mutagenesis studies aimed at addressing the contribution of salt bridges to protein stability using methods such as differential scanning calorimetry and chemical denaturation.

Conclusion

We have successfully eliminated the iron center in hyperthermophilic rubredoxin and created a small protein that displays reversible folding. The PFRD-XC4 variant has a melting temperature of 82 °C, a thermodynamic stability of 3.2 kcal mol^{-1} at 1 °C, and NMR chemical shifts that are similar to those of the wild-type protein. This variant should provide a tractable model system for studying the thermodynamic origins of protein hyperthermostability.

Acknowledgment. We thank M. K. Eidness for the wild-type *Pyroccocus furiosus* rubredoxin gene used in this study, S. M. Malakauskas, S. Ross, and C. Sarisky for technical assistance and discussions, and B. I. Dahiyat for discussions. The work was supported by the Howard Hughes Medical Institute (S.L.M.) and a NIH training grant (P.S.).

JA9834780

(40) Blake, P.; Park, J.; Zhou, Z.; Hare, D.; Adams, W. W. M.; Summers, M. *Protein Sci.* **1992**, 1508−1521.

(41) Koradi, R.; Billeter, M.; Wüthrich, K. *J. Mol. Graph.* **1996**, *14*, 51.

(42) Blake, P.; Park, J.; Bryant, F.; Aono, S.; Magnuson, J.; Eccleston, E.; Howard, J.; Summers, M.; Adams, M. *Biochemistry* **1991**, *30*, 5−10895.